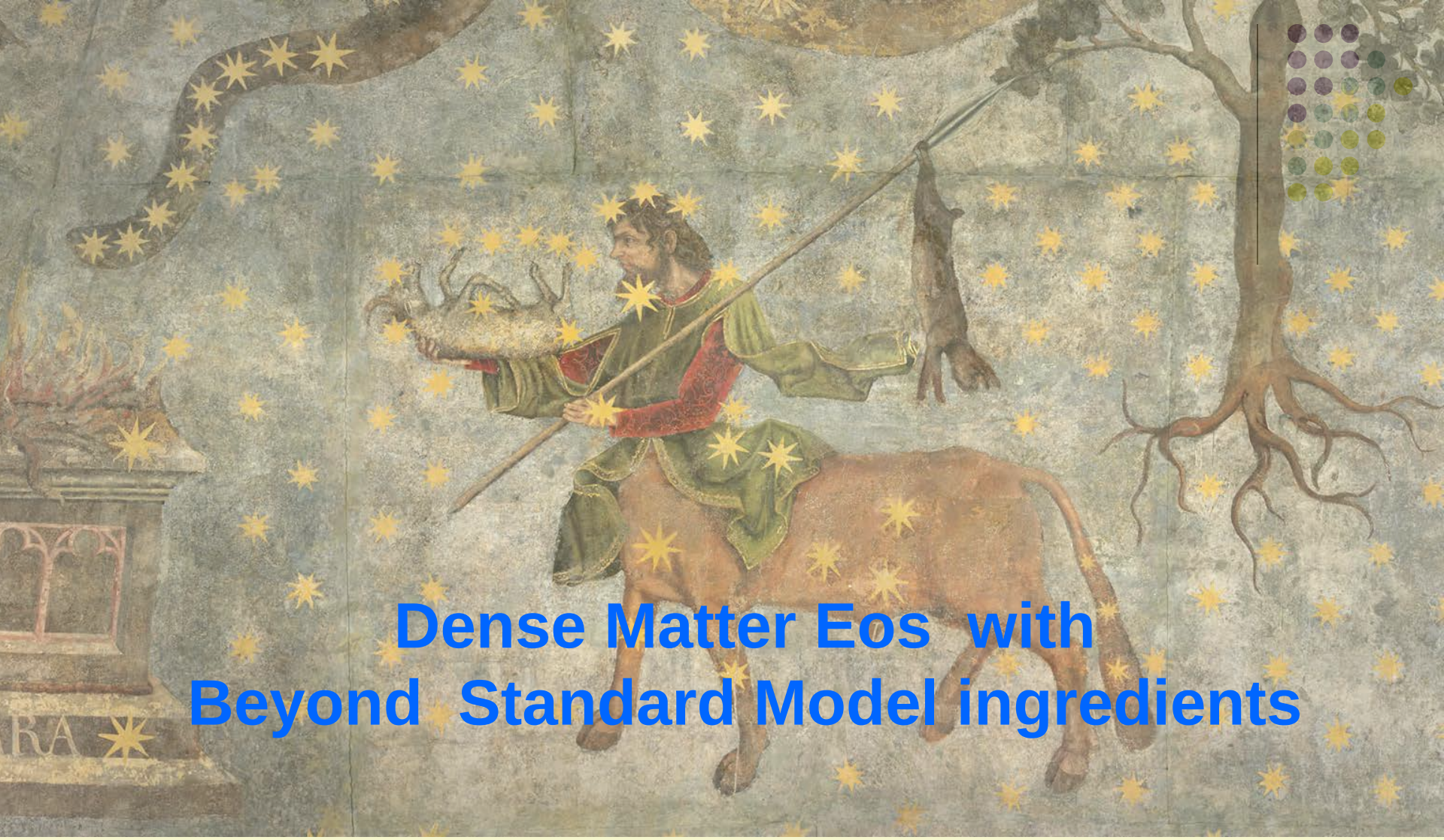

Dense Matter Eos with Beyond Standard Model ingredients

Ángeles Pérez-García

mperezga@usal.es

Department of Fundamental Physics
University of Salamanca, Spain

VNiVERSiDAD D SALAMANCA
CAMPUS DE EXCELENCIA INTERNACIONAL

800 AÑOS
1218 - 2018

MultiDark
Multimessenger Approach for Dark Matter Detection

Grupo de Astrofísica Nuclear & Astroparticulas

Evolutionary tale

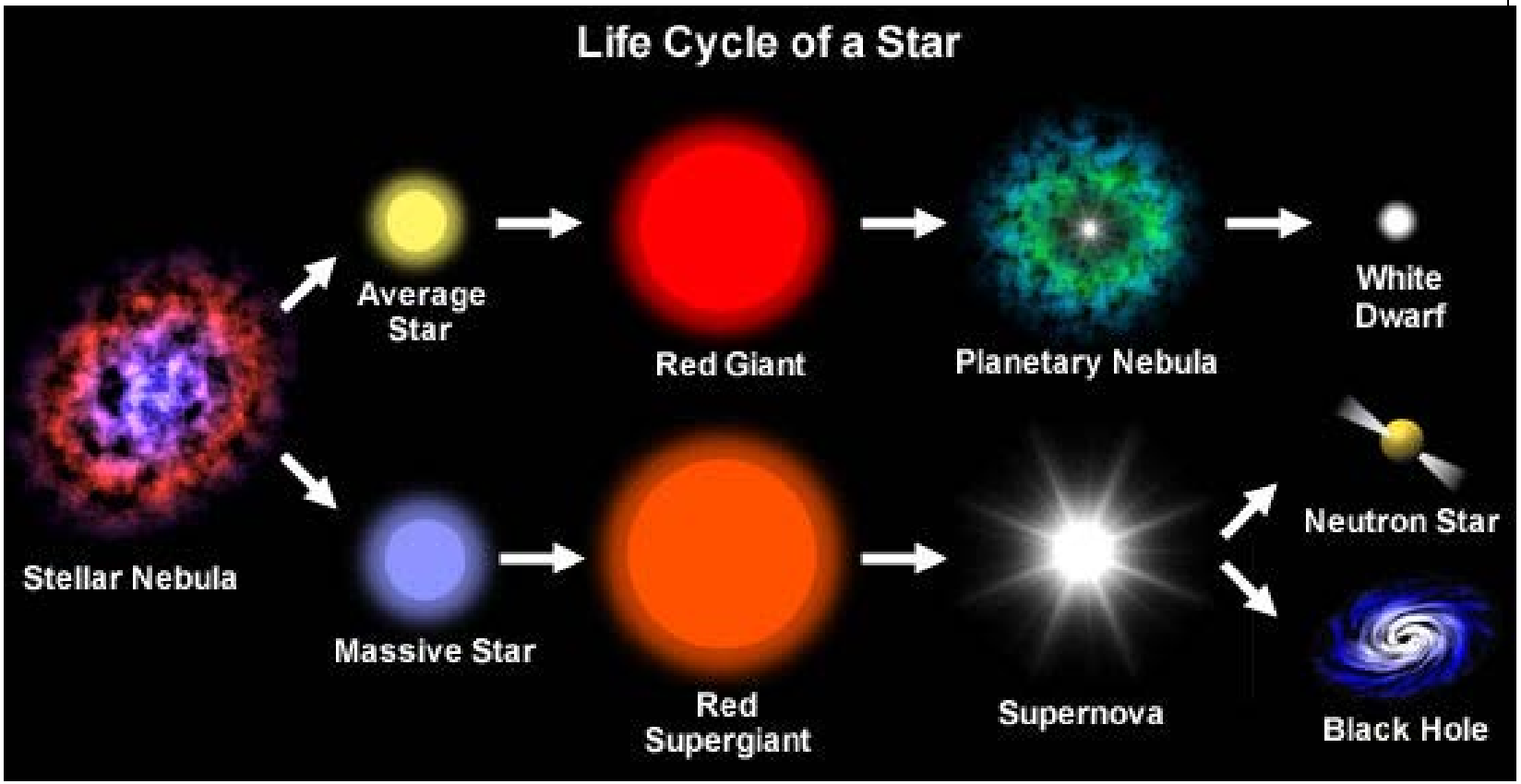

Stellar progenitors in the massive range beyond 8 solar masses are believed to undergo a SN explosion

Standard stellar evolution: SN events produce a compact massive object i.e. Neutron star, Black hole and perhaps other exotic compact stars.

Stellar interior: interplay of hadronic, weak, EM and gravitational interactions

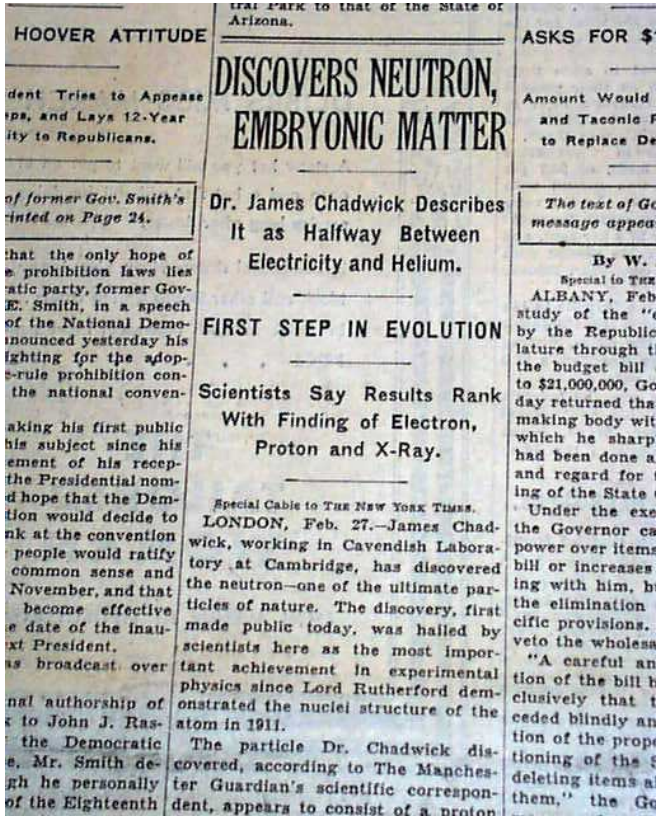

HOOVER ATTITUDE

dent Tries to Appease ps, and Lays 12-Year ity to Republicans.

of former Gov. Smith's inted on Page 24.

hat the only hope of e prohibition laws lies atic party, former Gov- E. Smith, in a speech of the National Demo- nounced yesterday his ighting for the adop- e-rule prohibition con- the national conven-

aking his first public his subject since his ement of his recep- the Presidential nom- d hope that the Dem- tion would decide to nk at the convention people would ratify common sense and November, and that become effective e date of the inau- xt President. as broadcast over

nal authorship of to John J. Ras- the Democratic e. Mr. Smith de- gh he personally of the Eighteenth

trial Park to that of the State of Arizona.

DISCOVERS NEUTRON, EMBRYONIC MATTER

Dr. James Chadwick Describes It as Halfway Between Electricity and Helium.

FIRST STEP IN EVOLUTION

Scientists Say Results Rank With Finding of Electron, Proton and X-Ray.

Special Cable to THE NEW YORK TIMES.

LONDON, Feb. 27.—James Chadwick, working in Cavendish Laboratory at Cambridge, has discovered the neutron—one of the ultimate particles of nature. The discovery, first made public today, was hailed by scientists here as the most important achievement in experimental physics since Lord Rutherford demonstrated the nuclei structure of the atom in 1911.

The particle Dr. Chadwick discovered, according to The Manchester Guardian's scientific correspondent, appears to consist of a proton

ASKS FOR $

Amount Would and Taconic to Replace De

The text of Gc message appea

By W. Special to THE ALBANY, Feb study of the " by the Republic lature through t the budget bill to $21,000,000, Gc day returned tha making body wit which he sharp had been done a and regard for ing of the State Under the exe the Governor ca power over items bill or increases ing with him, b the elimination cific provisions. veto the wholesa "A careful an tion of the bill h clusively that t ceded blindly an tion of the prop tioning of the deleting items a them," the Ge

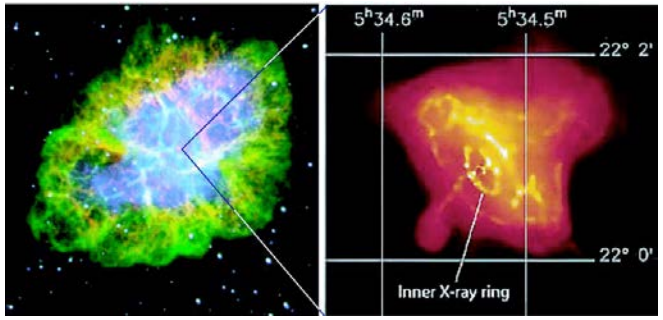

Crab V & X-rays (CHANDRA)

Rutherford predicted the neutron in 1920, Chadwick discovers it in 1932.

Chandrasekhar predicts the maximum WD mass supported by electrons in 1931 to be 1.4M Msun

Baade & Zwicky in 1934: "With all reserve we advance the view that a Supernova represents the transition of an ordinary star into a new form of star, the neutron star, which would be the end point of stellar evolution. Such a star may possess a very small radius and an extremely high density."

SN mechanism remains yet uncertain involving: weak messengers (neutrinos), EM radiation (photons) and gravitational waves.

Attending to further hints, other BSM astroparticles may be around the corner (ALPs, strangelets, steriles, wimps/simps..)

SN in transient sky: luminous events

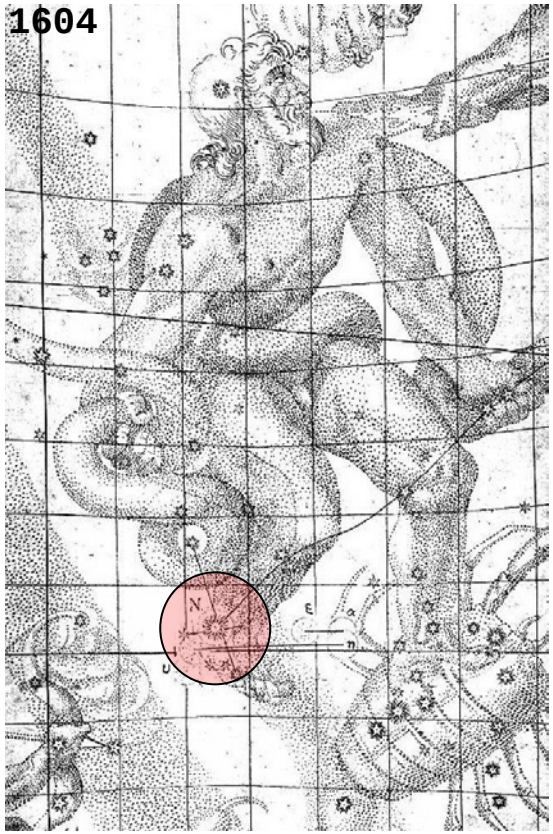

Some can be observed by naked eye for days.

Typically luminosity is 10^{10} L_sun, similar to that of Galaxy.

Nobel prizes with SN involvement: 1974 (pulsars), 2002 (neutrino astronomy), 2011 (SN ladder and cosmic expansion)

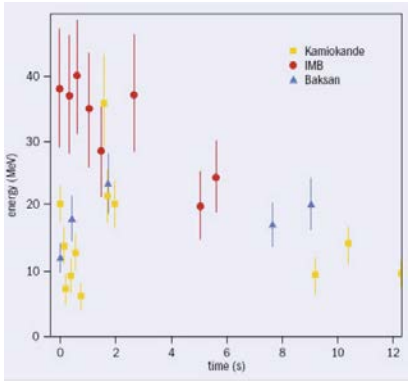

Neutrino role in the SN mechanism

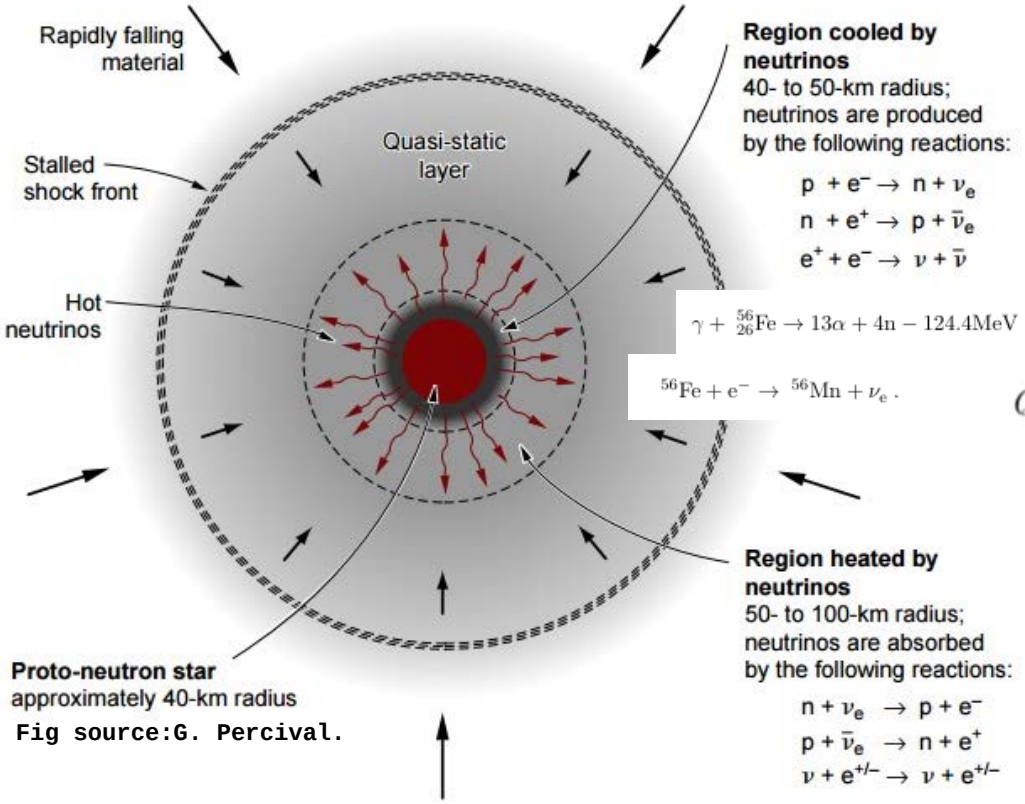

Fig source:G. Percival.

The delayed neutrino-driven SN mechanism is sensitive to a delicate competition of neutrino cooling between the neutrino sphere and the so-called 'gain radius'

$$Q_\nu^- \approx 145 \left(\frac{k_B T}{2\,\mathrm{MeV}}\right)^6 \left[\frac{\mathrm{MeV}}{\mathrm{s}\cdot N}\right]$$

. . . . . .

$$Q_\nu^+ \approx 110 \cdot \left(\frac{L_{\nu_e,52}\langle\epsilon^2_{\nu_e,15}\rangle}{r_7^2\,\langle\mu\rangle_{\nu_e}} Y_n + \frac{L_{\bar{\nu}_e,52}\langle\epsilon^2_{\bar{\nu}_e,15}\rangle}{r_7^2\,\langle\mu\rangle_{\bar{\nu}_e}} Y_p\right) \left[\frac{\mathrm{MeV}}{\mathrm{s}\cdot N}\right]$$

between the gain radius and the shock.

Absorption, emission, scattering, bremsstrahlung are the main processes driving the neutrino transport.

Only in case additional instabilities appear computatinal simulations find successful explosions

$(Z, A) \rightarrow (Z+1, A) + e^- + \bar{\nu}_e$

$(Z, A) + e^- \rightarrow (Z-1, A) + \nu_e.$

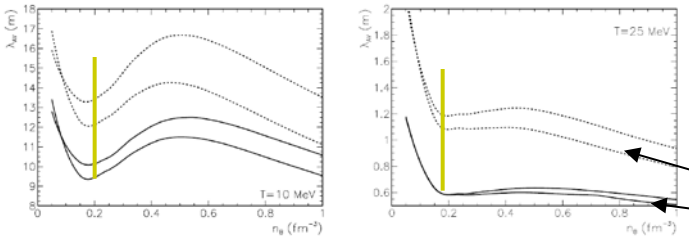

antinux_x
nu_x (PRC'03 Horowitz& PG

Further understanding (& questions) from Computational Simulations

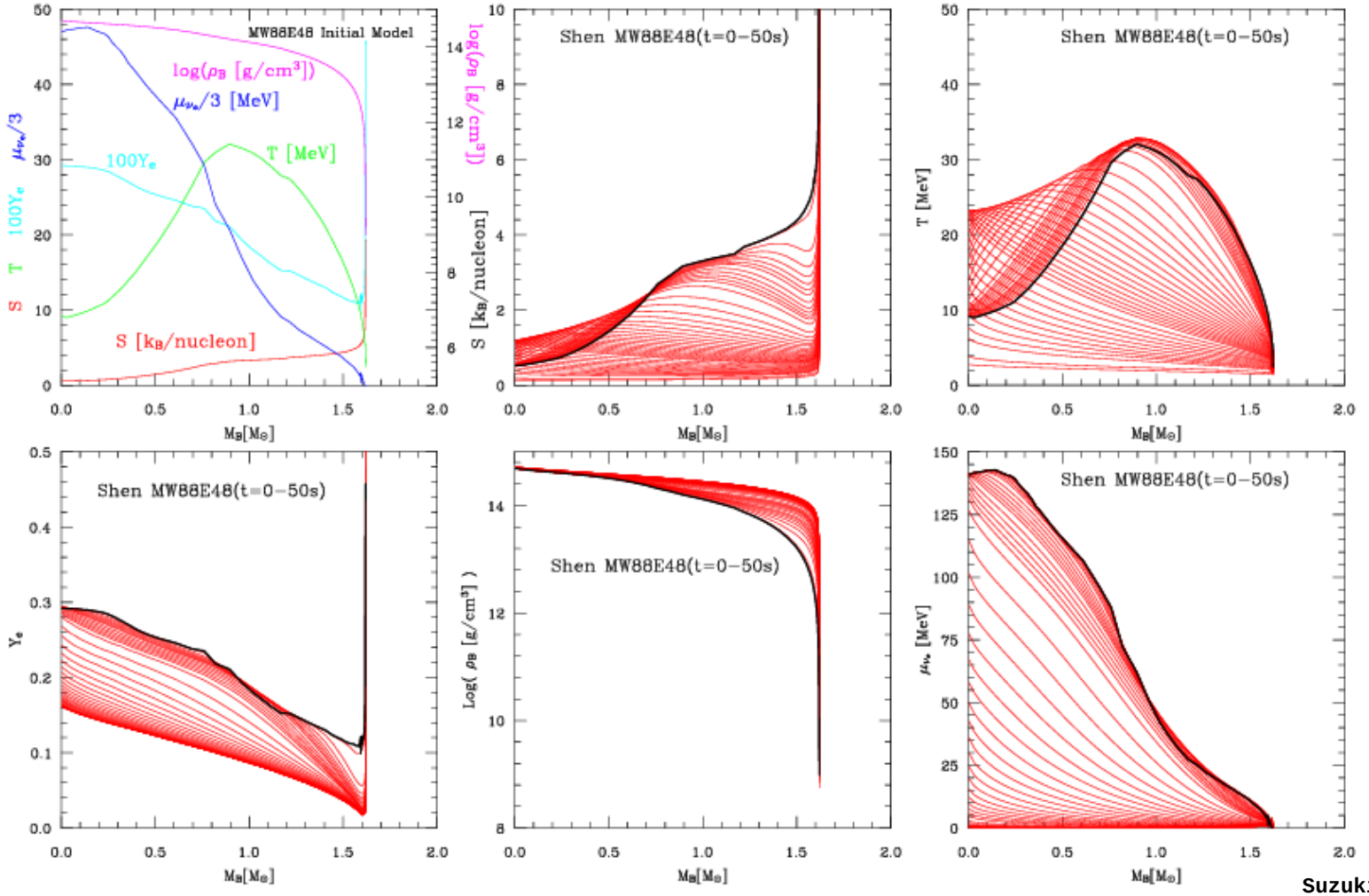

Suzuki, PTEP 2024

Fig. 4. Time evolution of the inner profiles of a proto-neutron star (model MW88E48). The upper left panel shows the initial profiles of density $\rho_{\rm B}$, temperature T, electron fraction $Y_{\rm e}$, entropy S, and neutrino chemical potential $\mu_{\nu_{\rm e}}$ defined as $\mu_{\rm p} + \mu_{\rm e} - \mu_{\rm n}$. The other five panels show snapshots up to 50 s. The black lines depict the initial profiles.

Composition and conserved charges

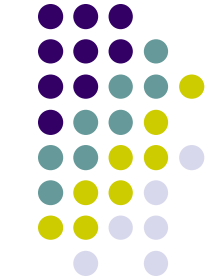

Late stages of evolution: Nuclear Statistical Equilibrium (NSE) i.e. independent of the rates for reactions mediated by the electromagnetic and strong interaction.

There is a first presupernova stage taken as initial

Later on SM conservation laws hold: weak decay, charge neutrality and conservation of (B,L) number must be imposed: e,mu,p,n,nu along with nuclei(Z,A). At low T

conditions	In-medium equilibrium
weak decay $n \to p + e + \bar{\nu}_e$	$\mu_n = \mu_p + \mu_e$
elec.charge neutrality $n_p = n_e + n_\mu$	$\mu_p = \mu_e + \mu_\mu$
conservation baryon number	$\rho_B = \rho_n + \rho_p$

Reaction	Equation
Electron emission	${}^A_Z X \to {}^A_{Z+1} X + e^- + \bar{\nu}_e$
Positron emission	${}^A_Z X \to {}^A_{Z-1} X + e^+ + \nu_e$
Electron capture	${}^A_Z X + e^- \to {}^A_{Z-1} X + \nu_e$
Positron capture	${}^A_Z X + e^+ \to {}^A_{Z+1} X + \bar{\nu}_e$
Electron annihilation	$e^- + e^+ \to \nu_e + \bar{\nu}_e$
Electron annihilation	$e^- + e^+ \to \nu + \bar{\nu}$
Neutrino capture	${}^A_Z X + {}^{(-)}_{\nu_e} \to {}^A_{Z\mp1} X + e^\pm$
$e^-\nu$ scattering	$e^- + {}^{(-)}_{\nu_e} \to e^- + {}^{(-)}_{\nu_e}$
$e^-\nu$ scattering	$e^\pm + {}^{(-)}_{\nu_e} \to e^\pm + {}^{(-)}_{\nu_e}$
Neutrino scattering	${}^A_Z X + {}^{(-)}_{\nu} \to {}^A_Z X + {}^{(-)}_{\nu}$

Weak process

$$\nu_\mu + \mu^\pm \leftrightarrows \mu'^\pm + \nu'_\mu$$
$$\bar{\nu}_\mu + \mu^\pm \leftrightarrows \mu'^\pm + \bar{\nu}'_\mu$$

$$\nu_\mu + e^- \leftrightarrows \mu^- + \nu_e$$
$$\bar{\nu}_\mu + e^+ \leftrightarrows \mu^+ + \bar{\nu}_e$$
$$\nu_\mu + \mu^+ \leftrightarrows e^+ + \nu_e$$
$$\bar{\nu}_\mu + \mu^- \leftrightarrows e^- + \bar{\nu}_e$$

Chemical potentials include protons, neutrons, electrons and muons along with neutrinos and their antiparticles if early trapped. Finite T antiparticles play a role i.e $Y_e = n_e^- - n_e^+$ **(neutrino free). Also possibly hyperons or other resonances. EoS description must capture this rich environment NSE used for around 1000 nuclear species and the relativistic (or not) mean field models for the unbound nucleons.**

Low density EoS: from inner to outer crust

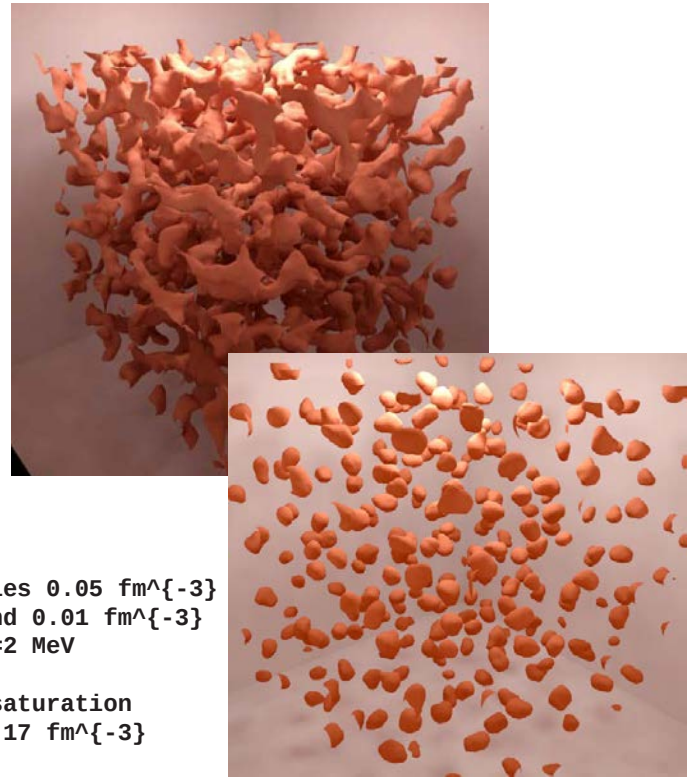

At densities 0.05 fm^{-3} (above) and 0.01 fm^{-3} (right) T=2 MeV

(typical saturation density 0.17 fm^{-3}

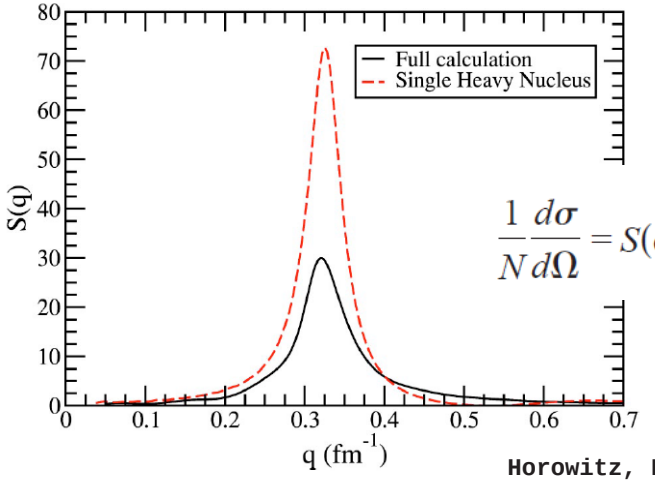

$$\frac{1}{N}\frac{d\sigma}{d\Omega} = S(\mathbf{q})\frac{G_F^2 E_\nu^2}{4\pi^2}\frac{1}{4}(1+\cos\theta).$$

Horowitz, PG et al PRC'04

FIG. 23. (Color online) Neutron static structure factor $S(q)$ as a function of the momentum transfer q at a density of $\rho = 0.025$ fm^{-3} (black solid line). Also shown (red dashed line) is the prediction from the ion static structure factor in Fig. 21 including the square of the cluster form factor, as explained in the text.

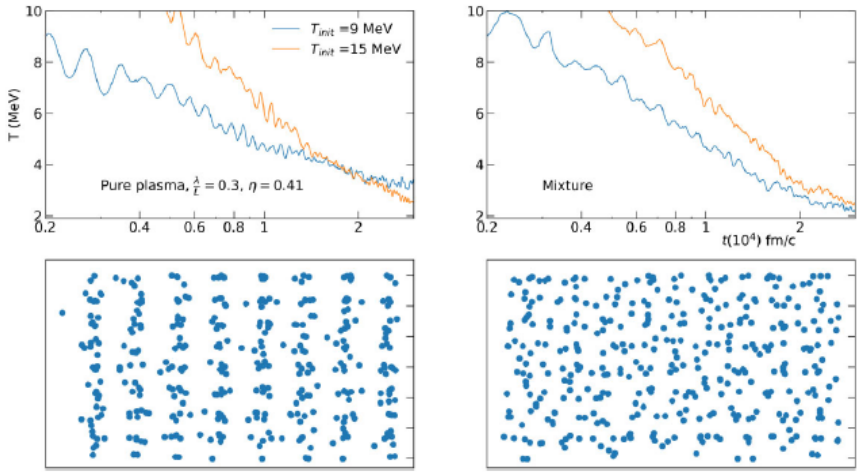

Effects of warm ion mixtures is key to understand effects of cooling.

Anomalous thermal relaxation of plasmas arise so that form factor decrease as ordered configuration dissolve.

Barba, Albertus, PG MNRAS '25

Figure 4. Top panel: Temperature $T(t)$ for a pure sample with $(Z, A) = (38, 128)$ (left) versus a mixture in which 40 percent of the original ions have been

Elastic and plastic crust properties

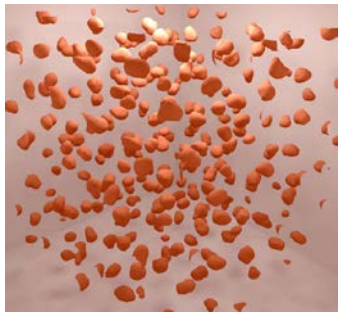

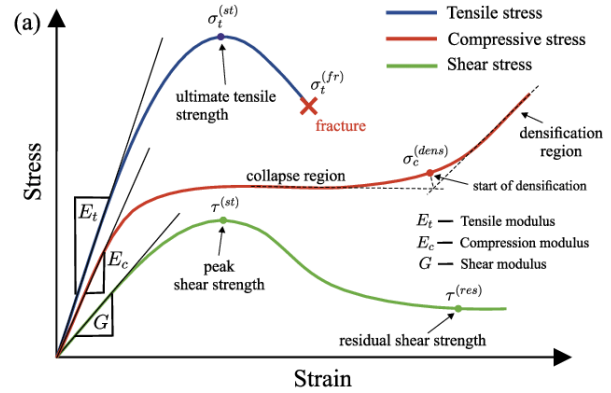

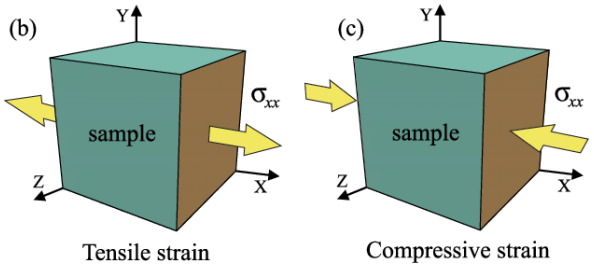

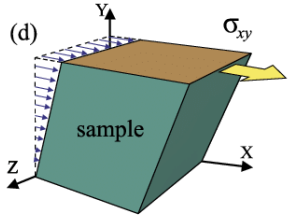

Elastic and plastic regions are poorly known. Tensile and Shear deformations are key to understand GW emission and KN ejecta.

Barba, Albertus and PG submitted

$$h_0 = \frac{16\pi^2 G I_{zz} f^2}{c^4 d} \epsilon.$$

Owen+'15

$$\epsilon_{\max} = 3.4 \times 10^{-7} \left(\frac{\epsilon_{\max}}{10^{-2}}\right) \left(\frac{1.4\,M_\odot}{M}\right)^{2.2} \left(\frac{R}{10\,\mathrm{km}}\right)^{4.26} \left[1 + 0.7\left(\frac{M}{1.4\,M_\odot}\right)\left(\frac{10\,\mathrm{km}}{R}\right)\right]^{-1}$$

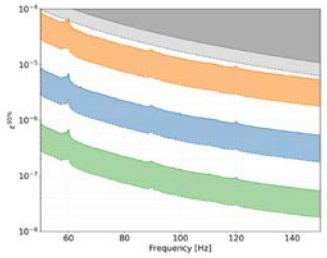

Covas+24

(Z,A)=28,138 nI=1e-6 fm^{-3}

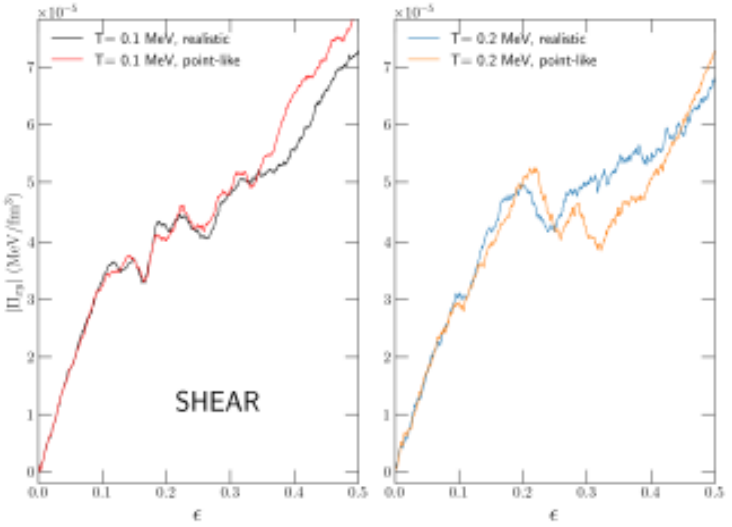

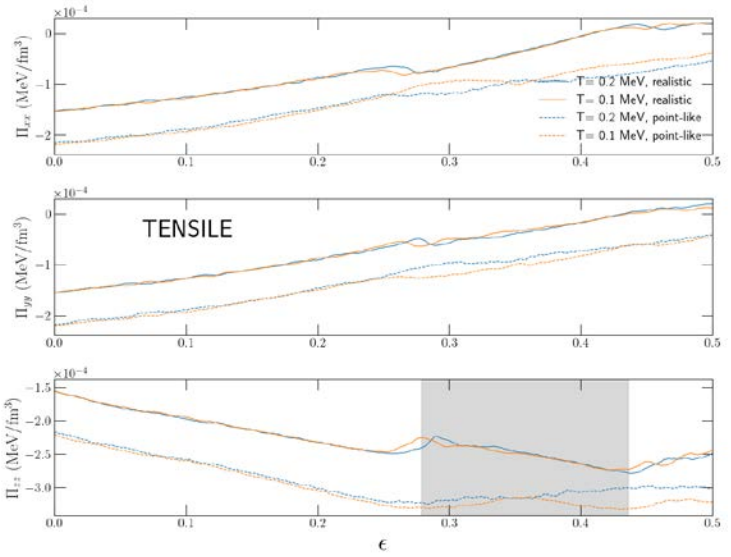

Elastic and plastic crust : B field

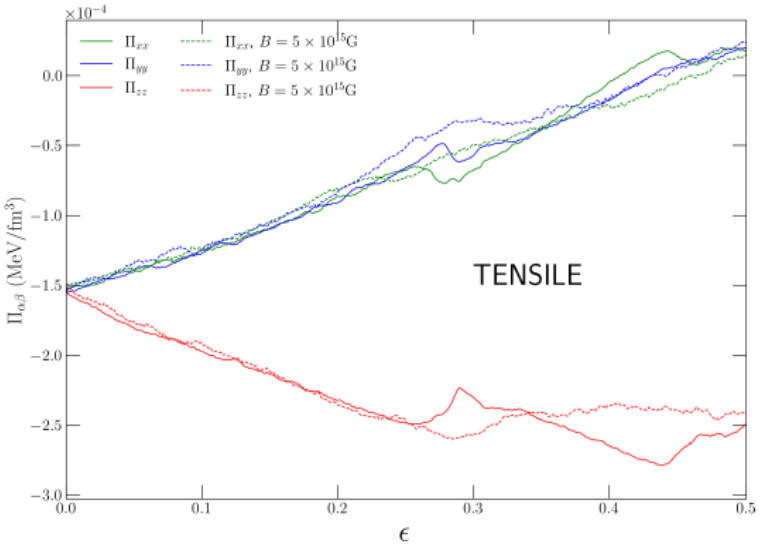

OCP (Z,A)=28,138 nI=1e-6 fm^{-3}
Murarka et al 2020

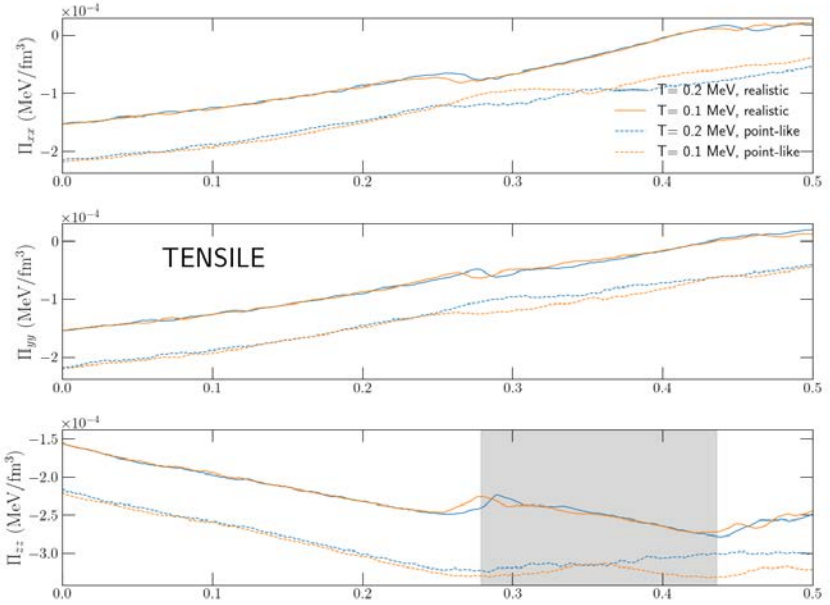

Elastic and plastic regions are different in case B field is present tending to make crust more robust.

Ewald sums and finite size ions screened by e sea

Barba, Albertus and PG submitted

$$\Pi^{\text{real}}_{\alpha\beta} = \frac{1}{2V}\sum_{i,j\neq i=1}^{\cdots}\left(F^{\text{real}}_{ij,\alpha}\, r_{ij,\beta} + F^{\text{real}}_{ij,\beta} r_{ij,\alpha}\right)$$

$$\Pi^{\text{recip}}_{\alpha\beta} = \frac{1}{2}\sum_{\vec{k}\neq 0}^{\infty}\sum_{i,j}^{N_I}\frac{4\pi Z_i Z_j e^2}{V^2\left(k^2+\frac{1}{\lambda_e^2}\right)} e^{\frac{-k^2}{4}\left(\frac{1}{a_i}+\frac{1}{\alpha_{\text{Ew}}}\right)} e^{i\vec{k}\cdot(\vec{r}_i-\vec{r}_j)}\times$$

$$\left\{\delta_{\alpha\beta} - 2\left[\frac{1}{4}\left(\frac{1}{a_i}+\frac{1}{\alpha_{\text{Ew}}}\right)+\frac{1}{\left(k^2+\frac{1}{\lambda_e^2}\right)}\right]k_\alpha k_\beta\right\}$$

$$\Pi^{\text{volume}}_{\alpha\beta} = -\frac{2\pi\delta_{\alpha\beta}}{V^2}\sum_{i=1}^{N_I}\sum_{j=1}^{N_I} Z_j e\int_0^\infty r'^2\phi_{\text{short-range,i}}(r')\,dr'.$$

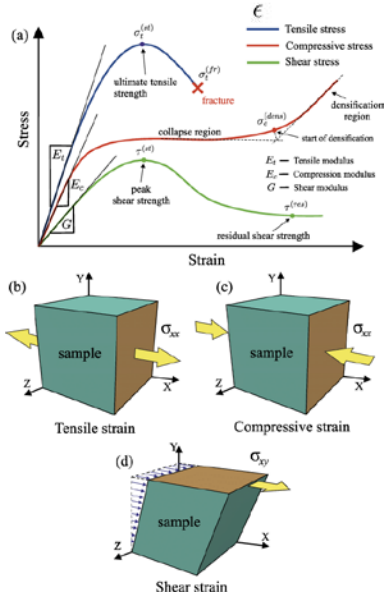

EoS based on SM fermion+cluster+meson fields

In the dense stellar core after the SN explosion high T of dozens of MeV drive system to a mixture of baryons, leptons. Relativistic field theories are well-suited to describe this system with EM fields Example: Shen EoS

$$\begin{aligned}\mathcal{L}_{RMF} &= \bar{\psi}\left[i\gamma_\mu\partial^\mu - M - g_\sigma\sigma - g_\omega\gamma_\mu\omega^\mu - g_\rho\gamma_\mu\tau_a\rho^{a\mu} - e\gamma_\mu\frac{1-\tau_3}{2}A^\mu\right]\psi \\ &+\frac{1}{2}\partial_\mu\sigma\partial^\mu\sigma - \frac{1}{2}m_\sigma^2\sigma^2 - \frac{1}{3}g_2\sigma^3 - \frac{1}{4}g_3\sigma^4 \\ &-\frac{1}{4}W_{\mu\nu}W^{\mu\nu} + \frac{1}{2}m_\omega^2\omega_\mu\omega^\mu + \frac{1}{4}c_3\left(\omega_\mu\omega^\mu\right)^2 \\ &-\frac{1}{4}R^a_{\mu\nu}R^{a\mu\nu} + \frac{1}{2}m_\rho^2\rho^a_\mu\rho^{a\mu} - \frac{1}{4}F_{\mu\nu}F^{\mu\nu},\end{aligned}$$

Shen et al NPA'98, Shen et al ApJ TM1'11

$$\begin{aligned}\varepsilon = &\sum_{i=p,n}\frac{1}{\pi^2}\int_0^\infty dk\,k^2\sqrt{k^2+M^{*2}}\left(f^k_{i+}+f^k_{i-}\right) \\ &+\frac{1}{2}m_\omega^2\omega^2+\frac{3}{4}c_3\omega^4+\frac{1}{2}m_\rho^2\rho^2 \\ &+\frac{1}{2}m_\sigma^2\sigma^2+\frac{1}{3}g_2\sigma^3+\frac{1}{4}g_3\sigma \quad +3\Lambda_v\left(g_\omega^2\omega^2\right)\left(g_\rho^2\rho^2\right),\end{aligned}$$

$$\begin{aligned}P = &\sum_{i=p,n}\frac{1}{3\pi^2}\int_0^\infty dk\,k^2\frac{k^2}{\sqrt{k^2+M^{*2}}}\left(f^k_{i+}+f^k_{i-}\right) \\ &-\frac{1}{2}m_\sigma^2\sigma^2-\frac{1}{3}g_2\sigma^3-\frac{1}{4}g_3\sigma^4 \\ &+\frac{1}{2}m_\omega^2\omega^2+\frac{1}{4}c_3\omega^4+\frac{1}{2}m_\rho^2\rho^2 \\ &+\Lambda_v\left(g_\omega^2\omega^2\right)\left(g_\rho^2\rho^2\right).\end{aligned}$$

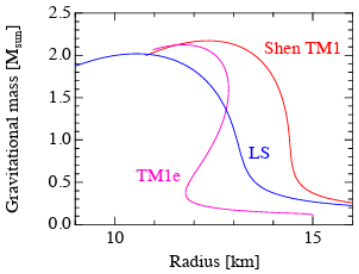

Sumiyoshi'21

RMF nucleon+ lepton gas

ideal

Nucleon gas+ ion mixture

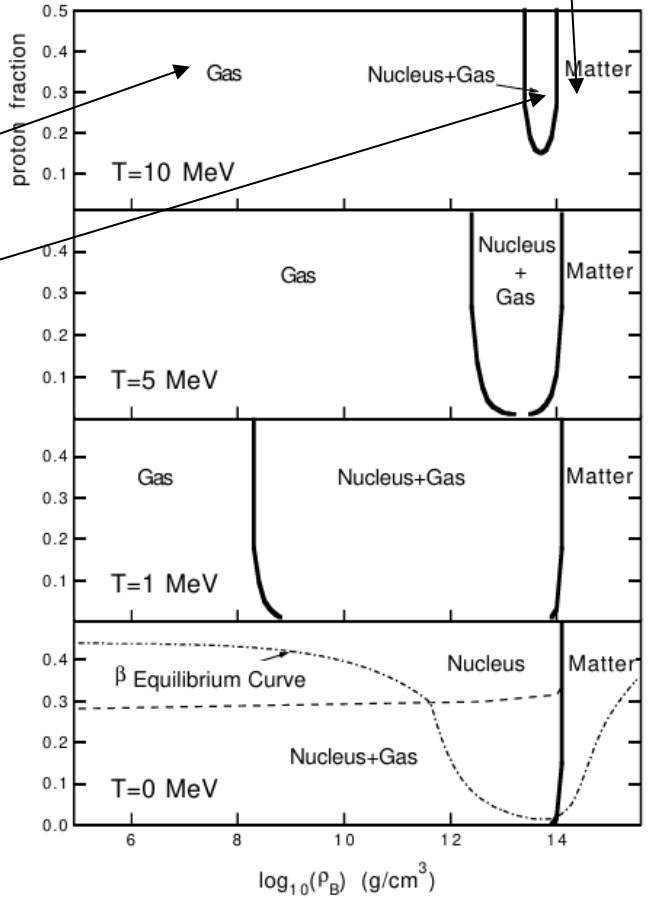

But is this all? Perhaps not. .
BSM dark matter and dense matter EoS: a few examples

$$\mathcal{L}_{\mathcal{I}} = -i\frac{g_\chi}{\sqrt{2}} a\bar{\chi}\gamma_5\chi - ig_0\frac{g_f}{\sqrt{2}} a\bar{f}\gamma_5 f \,,$$

Coy DM from C. Boehm et al '14

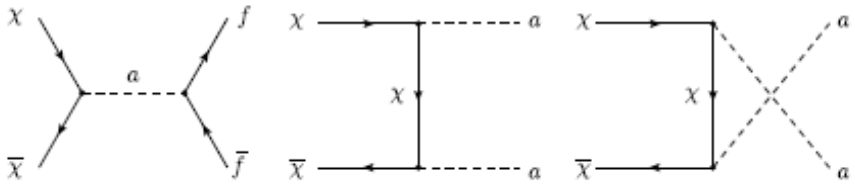

Cermeño, Perez-Garcia, Lineros, ApJ '18

$$m_\chi < m_{Higgs}; m_a < m_\chi$$

Model	m_χ [GeV]	m_a [GeV]	g_χ	g_0
A	0.1	0.05	7.5×10^{-3}	7.5×10^{-3}
B	1	0.05	1.2×10^{-1}	2×10^{-3}
C	30	1	6×10^{-1}	5×10^{-5}

Table 1: Parameters used Coy DM. Flavour-universal $g_f = 1$.

Cermeño, Pérez, Silk, PASA 34, e043(2017)

Massive progenitors accumulate thermalized DM, most likely from scattering SI or SD interactions or direct production. Tiny DM amount

Hybrid stars with dark content are indeed possible if CS is above critical threshold

$$r_{th}(t) = \left(\frac{3k_B T_c(t)}{2\pi G\rho_c(t) m_\chi}\right)^{1/2},$$

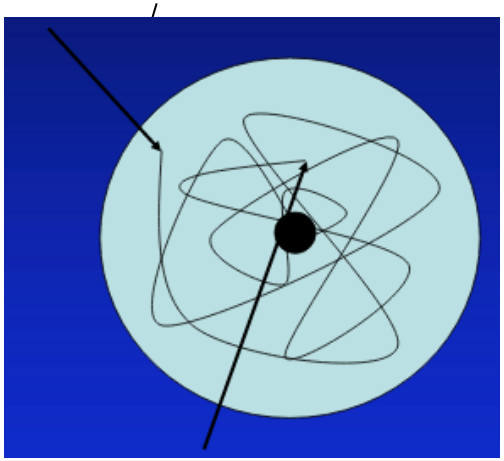

$$XX \to \nu\bar{\nu}$$

$$XX \to aa, a \to \nu\bar{\nu}$$

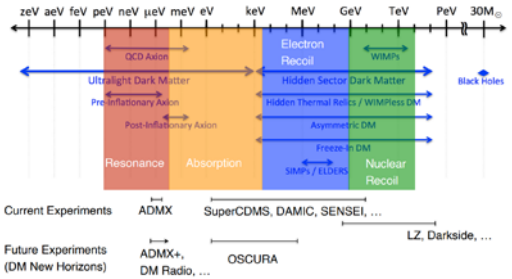

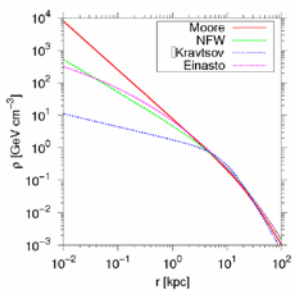

Fermion DM : two fluid solution from core to halo.

$$\mathcal{L}_{\rm SIDM,int} \supset -g_V \bar{\chi}\gamma^\mu \chi V_\mu + g_S \bar{\chi} S \chi,$$

$$\frac{\sigma_{\rm SI}}{m_\chi} = \frac{3y^4 g^4}{16\pi m_\chi^3}.$$

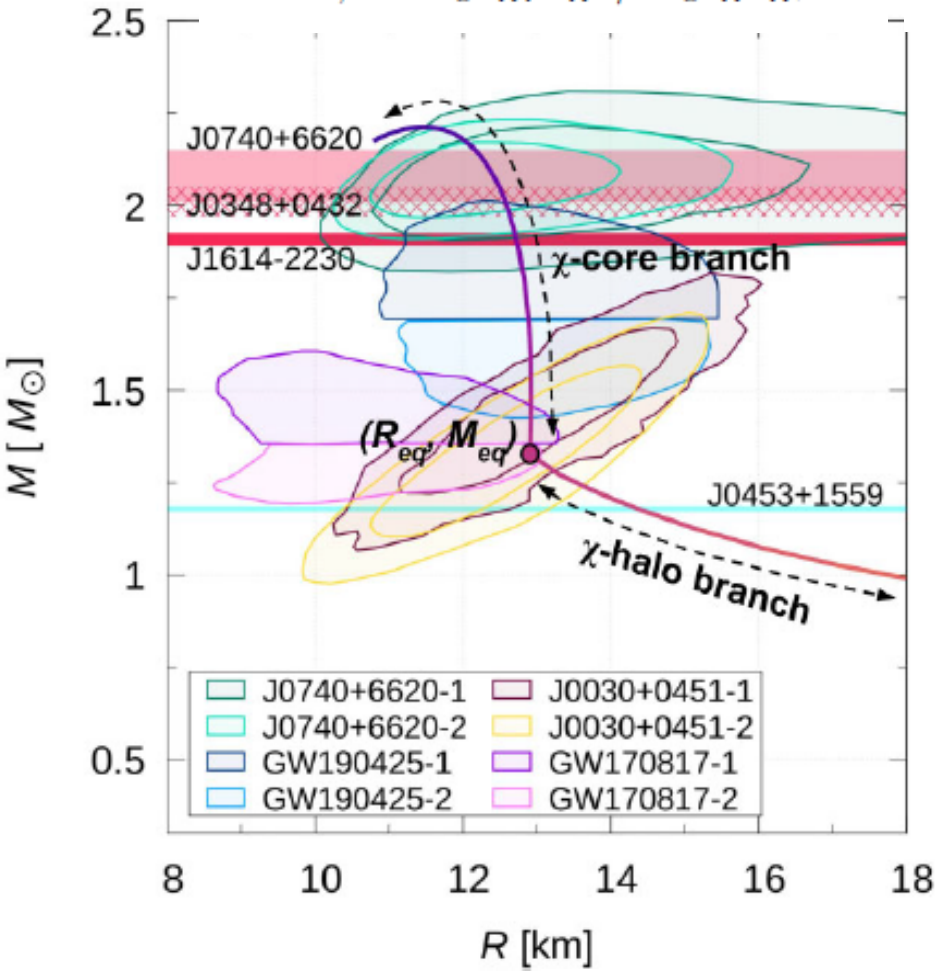

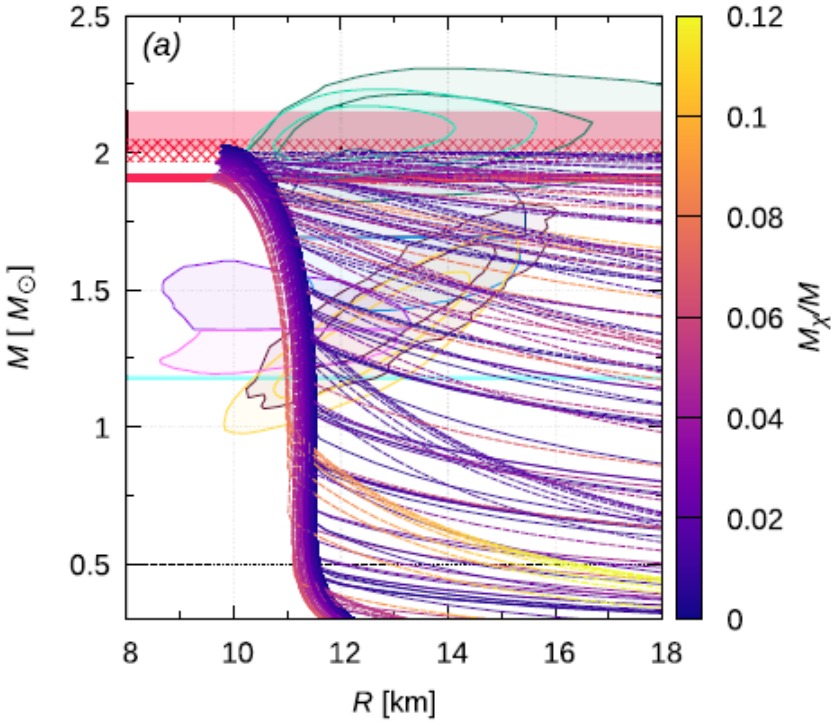

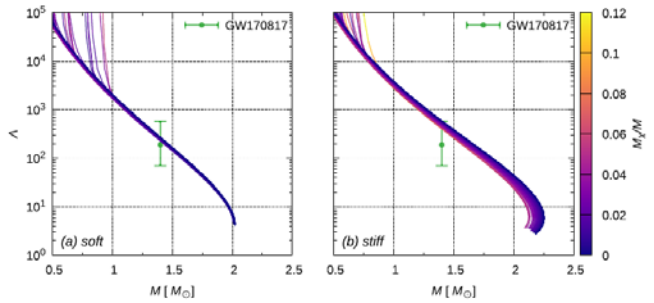

$$p(\rho) = K_i \rho^{\Gamma_i} + \Lambda_i,$$

$$\epsilon(\rho) = \frac{K_i}{\Gamma_i - 1}\rho^{\Gamma_i} + (1 + a_i)\rho - \Lambda_i,$$

Mariani, Albertus,PG+'24
Mukhop,Schaffner'16

Neutrino emissivity from DM

Early cooling by neutrinos may be influence by annihilation processes under the emissivity (energy per unit volume unit time) $12 \to 34$

$$Q_E = 4 \int d\Phi (E_1 + E_2) \, |\overline{\mathcal{M}}|^2 \, f(f_1, f_2, f_3, f_4)$$

with

$$d\Phi = \frac{d^3p_1}{2(2\pi)^3 E_1} \frac{d^3p_2}{2(2\pi)^3 E_2} \frac{d^3p_3}{2(2\pi)^3 E_3} \frac{d^3p_4}{2(2\pi)^3 E_4} (2\pi)^4 \delta^4(p_1 + p_2 - p_3 - p_4)$$

and matrix element $XX \to \nu\overline{\nu}$ $XX \to aa$

Neutrino emissivities from Coy DM have genuinely different T behavior than Modified URCA+ SM processes

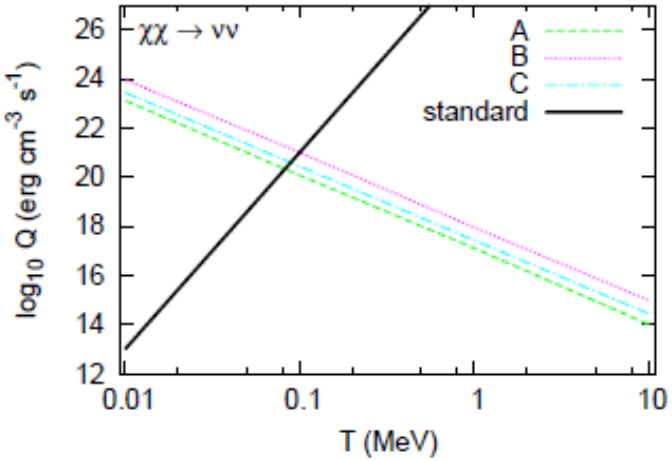

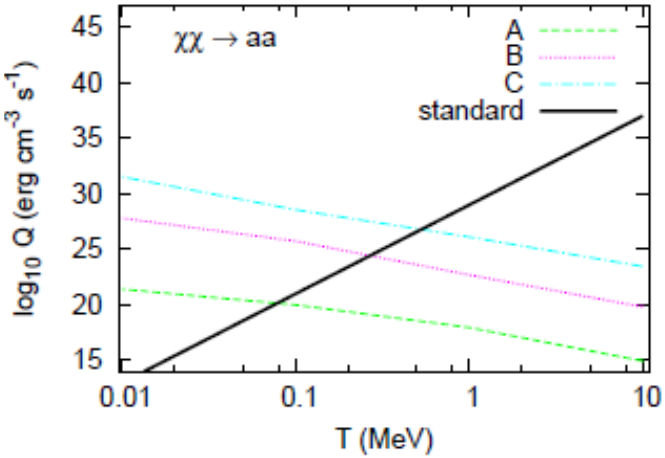

reaction $\chi\chi \to aa$ could provide emissivities $Q_E^{aa} \sim 4 \times 10^{22}$ erg cm^{-3} s^{-1} Higher than for the $Q_{MX1659-29} \sim 1.7 \times 10^{21}$ erg cm^{-3} s^{-1} for $T \sim 10^8$ K.

Channel	Model	$\log_{10} Q_0$	$N_{0,\chi}$
$\chi\chi \to \nu\nu$	A	17.3	4.1×10^{44}
$\chi\chi \to \nu\nu$	B	18	2.4×10^{44}
$\chi\chi \to \nu\nu$	C	17.6	5×10^{38}
$\chi\chi \to aa$	A	18	4.1×10^{44}
$\chi\chi \to aa$	B	22.5	2.4×10^{44}
$\chi\chi \to aa$	C	27	5×10^{38}

$$Q_E(T, N_\chi) = Q_0 \left(\frac{N_\chi}{N_{0,\chi}}\right)^2 \left(\frac{T}{1\,\mathrm{MeV}}\right)^{-3}$$

Cermeño, Perez-Garcia, Lineros ApJ '18

Neutrino emissivity: example from coy DM

Early cooling by neutrinos may be influence by annihilation processes under the emissivity (energy per unit volume unit time) $12 \to 34$

with

$$d\Phi = \frac{d^3p_1}{2(2\pi)^3 E_1}\frac{d^3p_2}{2(2\pi)^3 E_2}\frac{d^3p_3}{2(2\pi)^3 E_3}\frac{d^3p_4}{2(2\pi)^3 E_4}(2\pi)^4\delta^4(p_1+p_2-p_3-p_4)$$

and matrix element $XX \to \nu\overline{\nu}$ $XX \to aa$

Neutrino emissivities from Coy DM have genuinely different T behavior than Modified URCA+ SM processes

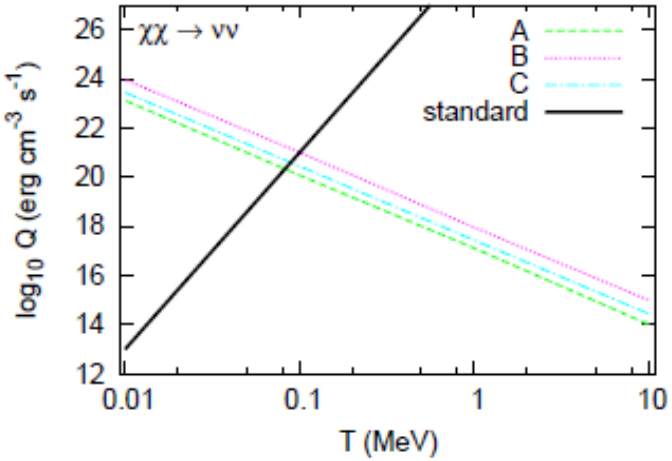

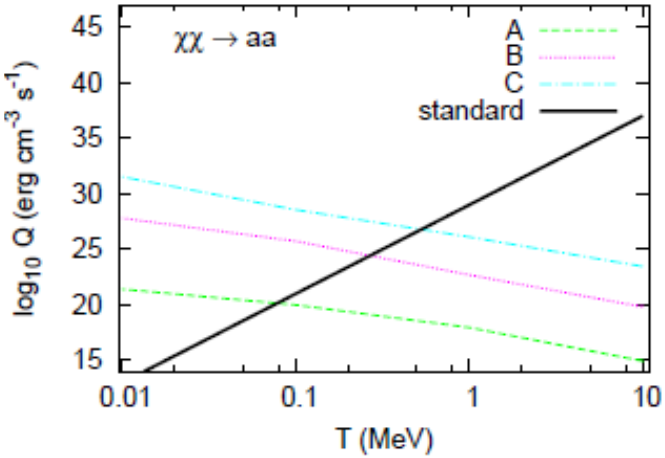

reaction $\chi\chi \to aa$ could provide emissivities $Q_E^{aa} \sim 4 \times 10^{22}$ erg cm^{-3} s^{-1} Higher than for the $Q_{MX1659-29} \sim 1.7 \times 10^{21}$ erg cm^{-3} s^{-1} for $T \sim 10^8$ K.

Channel	Model	$\log_{10}$ Q$_0$	$N_{0,\chi}$
$\chi\chi \to \nu\nu$	A	17.3	4.1×10^{44}
$\chi\chi \to \nu\nu$	B	18	2.4×10^{44}
$\chi\chi \to \nu\nu$	C	17.6	5×10^{38}
$\chi\chi \to aa$	A	18	4.1×10^{44}
$\chi\chi \to aa$	B	22.5	2.4×10^{44}
$\chi\chi \to aa$	C	27	5×10^{38}

$$Q_E(T, N_\chi) = Q_0 \left(\frac{N_\chi}{N_{0,\chi}}\right)^2 \left(\frac{T}{1\,\mathrm{MeV}}\right)^{-3}$$

Cermeño, Perez-Garcia, Lineros ApJ '18

Cooling behaviour in the NS for a LDM case

When considering the previous model in cooling calculations (SF and hadronic model)

$$\frac{e^{-\lambda-2\Phi}}{4\pi r^2}\frac{\partial}{\partial r}\left(e^{2\Phi}L\right) = -Q + Q_h - \frac{c_V}{e^{\Phi}}\frac{\partial T}{\partial t},$$

$$\frac{L}{4\pi\kappa r^2} = e^{-\lambda-\Phi}\frac{\partial}{\partial r}\left(Te^{\Phi}\right)$$

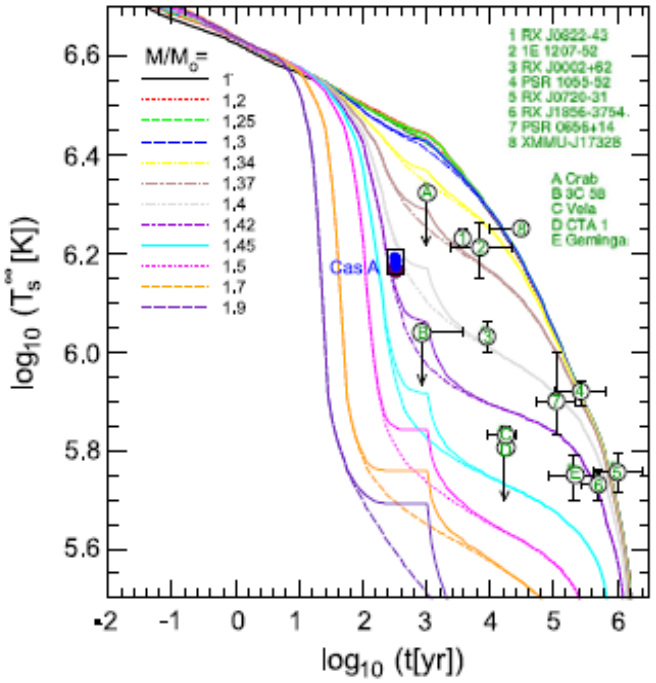

$$Q_h \equiv Q_{\chi\chi}(T) = 10^{\alpha}\left(\frac{T}{0.1\,\mathrm{MeV}}\right)^{-3}\ \mathrm{erg\,cm^{-3}\,s^{-1}},$$

with $19 < \alpha < 21$.

LDM m_x=100 MeV is considered

More massive NS could lead to a temporary Temperature plateau halt

Degeneracy for interpretation cooling with admixed DM or only SM processes

PG, Grigorian, Albertus, Barba, Silk, PLB 827 (2022)

SN EoS and DM as sterile neutrinos

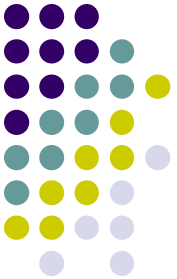

Yet another possibility BSM shows how sensitive SN EoS is

$$\mathcal{L}_{\rm eff} = \mu\, \bar{\nu}_h \sigma_{\mu\nu} \nu_h\, \partial^\mu A^\nu\,, \qquad \mu \approx e\, \frac{g_R^2}{16\pi^2}\, \frac{m_E}{M_R^2} \approx 10^{-6}\,{\rm GeV}^{-1}\,.$$

$$\mathcal{L}_{\rm eff} = \frac{1}{2}\, \mu_{\rm tr}\, \overline{\nu}_h\, \sigma_{\mu\nu}\, (1-\gamma_5)\, \nu\, \partial^\mu A^\nu + {\rm h.c.}\,, \qquad \mu_{\rm tr} \approx \sin\theta \mu \qquad \nu_h \to \nu\,\gamma$$

- **Active and sterile mixing** $N' = \cos\theta\, N + \sin\theta\, \nu \nu' = -\sin\theta\, N + \cos\theta\, \nu.$
- **We will assume the mixing is** $\sin^2\theta < 10^{-3}$ **in order not to conflict with cosmological bounds**
- **The dominant production channel will be electromagnetic** $e^+e^- \to \bar{\nu}_h \nu_h$

$$\frac{{\rm d}\sigma}{{\rm d}t} = \frac{\alpha\mu^2}{s^2 - 4sm_e^2} \left(-t + 2m_h^2 + m_e^2 - \frac{t^2 - 2(m_h^2 + m_e^2)t + (m_h^2 - m_e^2)^2}{s} \right)$$

- **Also active-sterile mixing** $\nu X \to \nu_h X$ **scattering** $\nu_h\, X \to \nu_h\, X$ **absorption**

Emissivity from steriles

Energy emissivity

$$Q_E(e^+e^- \to \bar{\nu}_h \nu_h) = \frac{dE}{dt dV}$$

$$Q_E = \frac{4}{(2\pi)^8} \int \frac{d^3p_1}{2E_1} \frac{d^3p_2}{2E_2} \frac{d^3p_3}{2E_3} \frac{d^3p_4}{2E_4} \delta^4(p_1+p_2-p_3-p_4)\,(E_1+E_2)\,|\bar{\mathcal{M}}|^2\, f(f_1,f_2,f_3,f_4)$$

$$|\bar{\mathcal{M}}(e^+e^- \to \bar{\nu}_h \nu_h)|^2 = 4e^2\mu_h^2 \left(-t + 2m_h^2 + m_e^2 - \frac{t^2 - 2(m_h^2+m_e^2)t + (m_h^2-m_e^2)^2}{s}\right)$$

The dense and hot medium

Albertus, Masip, PG, PLB'15

$$f_i(E) = \frac{1}{e^{(E-\mu_i)/T}+1}$$

$$\mu_{e-} = -\mu_{e+} 100\,\text{MeV}$$

$$T = 25\,\text{MeV}$$

Fit Energy emissivity

$$Q_E \approx 1.5 \times 10^{36} \left(\frac{\mu}{10^{-6}\,\text{GeV}^{-1}}\right)^2 \left(\frac{T}{25\,\text{MeV}}\right)^{7.4} e^{-\frac{m_h+\mu_e}{3T}} \frac{\text{erg}}{\text{s cm}^3}\,.$$

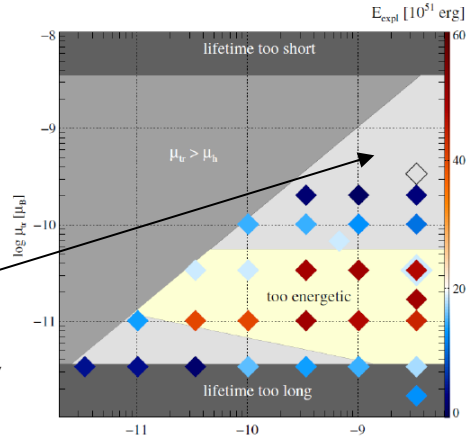

Light gray regions not excluded

Rembiasz, Obergaulinger, PG et al PRD'18

$m_h = 50 - 80\ \text{MeV}/c^2$

T	μ_e	Q_{50}	Q_{80}
5	20	$1.53656 \cdot 10^{26}$	$5.66121 \cdot 10^{21}$
5	40	$1.36192 \cdot 10^{26}$	$5.65149 \cdot 10^{21}$
5	60	$6.62017 \cdot 10^{25}$	$5.38001 \cdot 10^{21}$
5	80	$1.40457 \cdot 10^{25}$	$3.70775 \cdot 10^{21}$
5	100	$1.57973 \cdot 10^{24}$	$1.36088 \cdot 10^{21}$
5	120	$1.14701 \cdot 10^{23}$	$2.67659 \cdot 10^{20}$
5	140	$5.92976 \cdot 10^{21}$	$3.23395 \cdot 10^{19}$

T	μ_e	Q_{50}	Q_{80}
20	20	$5.91745 \cdot 10^{34}$	$1.46498 \cdot 10^{34}$
20	40	$5.40009 \cdot 10^{34}$	$1.40987 \cdot 10^{34}$
20	60	$4.55643 \cdot 10^{34}$	$1.29812 \cdot 10^{34}$
20	80	$3.52661 \cdot 10^{34}$	$1.12208 \cdot 10^{34}$
20	100	$2.51089 \cdot 10^{34}$	$8.99522 \cdot 10^{33}$
20	120	$1.65963 \cdot 10^{34}$	$6.67171 \cdot 10^{33}$
20	140	$1.02932 \cdot 10^{34}$	$4.59968 \cdot 10^{33}$

Stellar collapse and BSM trigger QCD EoS

SN core collapse involves high T and large densities in the inner core. There is a long-sought possibility of producing bubble nucleation
Self-annihilating DM act as a Trojan Horse mechanism and final state photon injection $XX \to q\bar{q} \to N\gamma$

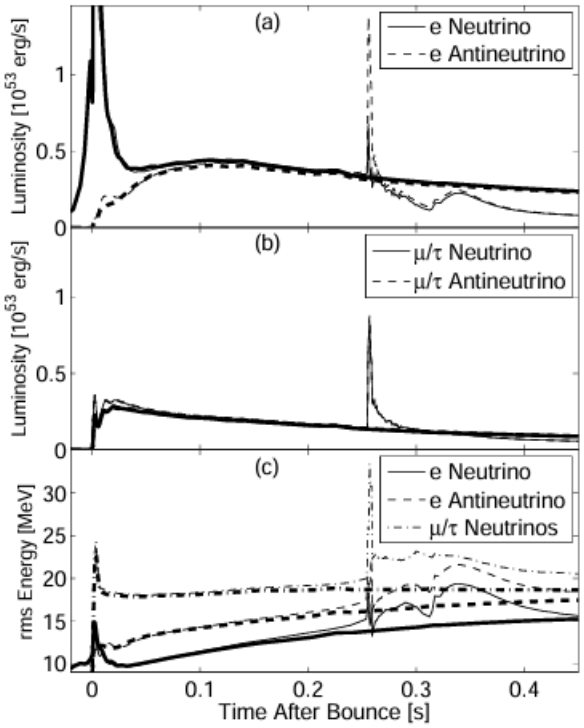

FIG. 2: Neutrino luminosities (a) and (b) and rms-energies (c) measured at 500 km distance for a 10 $M_\odot$ progenitor model. The results of the quark EoS *eos1* (thin lines) are compared to the results of the pure hadronic EoS [18] (thick lines). A second neutrino burst is clearly visible at $\sim$ 260 ms after bounce.

Sagert et al PRL'08

hadronic system could suffer a phase transition from a metastable phase (Hadron) to a more stable one (Quark-gluon) if right thermodynamical conditions

MIT Bag model required to be on the B=160 MeV^{-1}

Distinctive double neutrino burst.

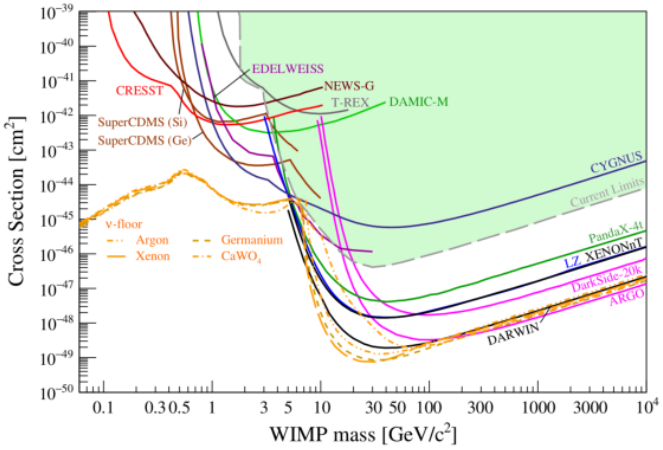

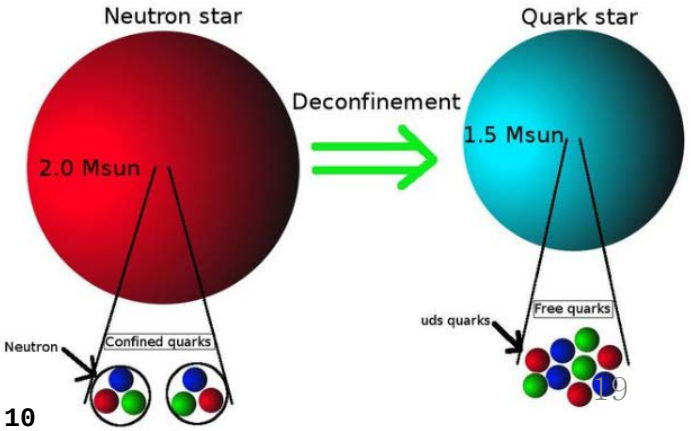

PG, Silk & Stone PRL'10

Confining potentials in LK theory

$$70 \leq B \leq 150\,\mathrm{MeV\,fm^{-3}}$$
$$10 \leq \sigma \leq 30\,\mathrm{MeV\,fm^{-2}}$$

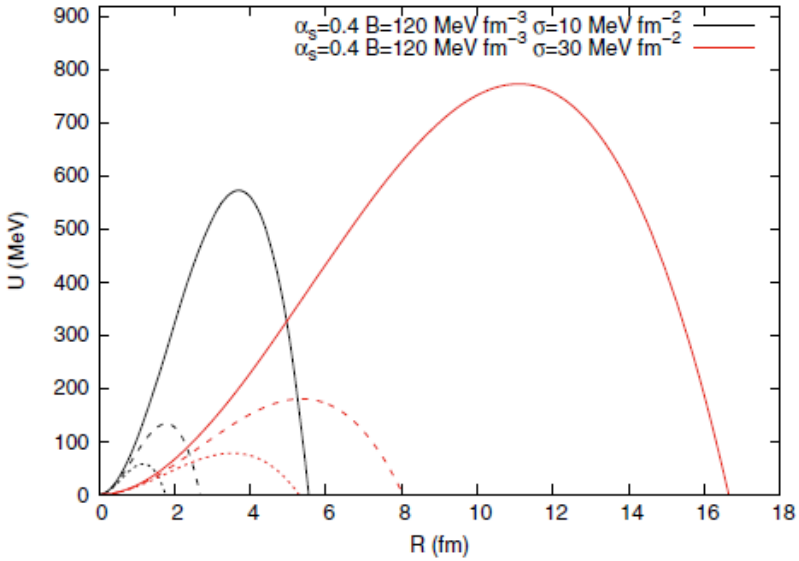

fm size bubbles

Potential barrier lower as pressure goes larger than transition density at $n_b|_H = 5.5 n_0$
QCD corrections drive smaller barriers.

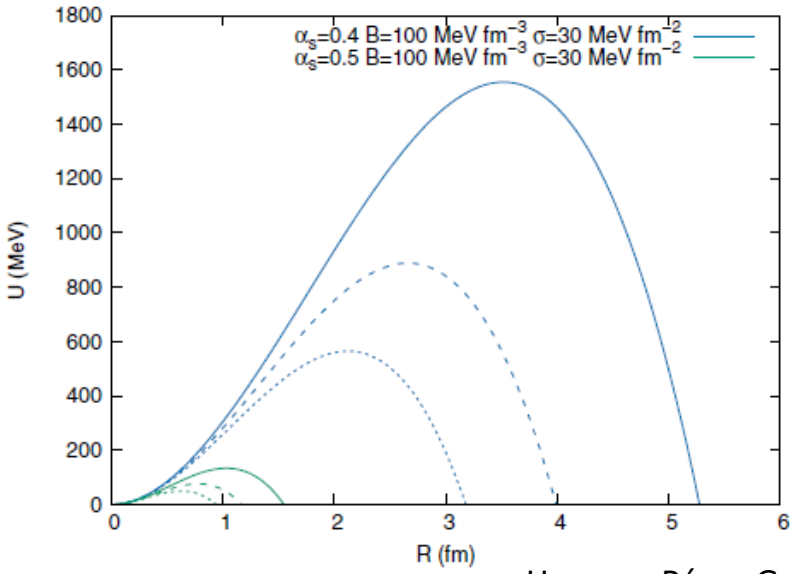

$$E = \frac{\xi m_\chi}{n_b 4\pi R^3} \qquad \xi \leq 0.6$$

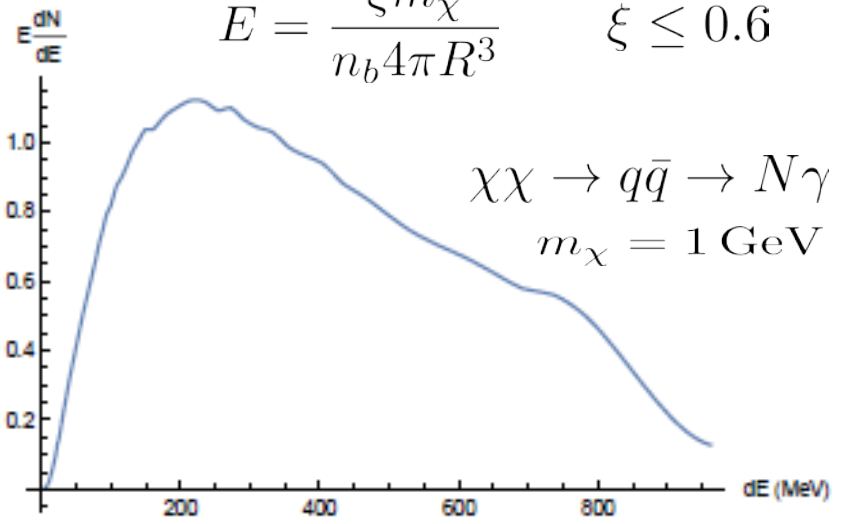

$$\chi\chi \to q\bar{q} \to N\gamma$$
$$m_\chi = 1\,\mathrm{GeV}$$

Herrero, Pérez-García, Silk and Albertus, PRD 100 (2019) 103019

Probability of induced nucleation

Oscillation frequency of the fundamental state

$$\nu_0^{-1} = \left.\frac{dI}{dE}\right|_{E=E_0}; \quad I(E) = \frac{2}{c}\int_{R_-}^{R_+} \sqrt{[2M(R)c^2 + E - U(R)]\,[U(R) - E]}\, dR$$

and the probability with (WKB approx)

$$p_0 = exp\left(-\frac{A(E)}{\hbar}\right);$$

The inject. energy per unit baryon charge inside the baryon bag determines the energetic level of confined Q content

$$E = \frac{\xi m_\chi}{n_b 4\pi R^3}$$

The number of nucleation centers is given by the stable bubble size

$$N_C = \frac{V_{th}}{V_B} \sim \left(\frac{r_{th}}{R_B}\right)^3.$$

and the bubble formation time $\tau^{-1} = \nu_0 p_0$
is corrected as $\tau_N = \tau / N_C$

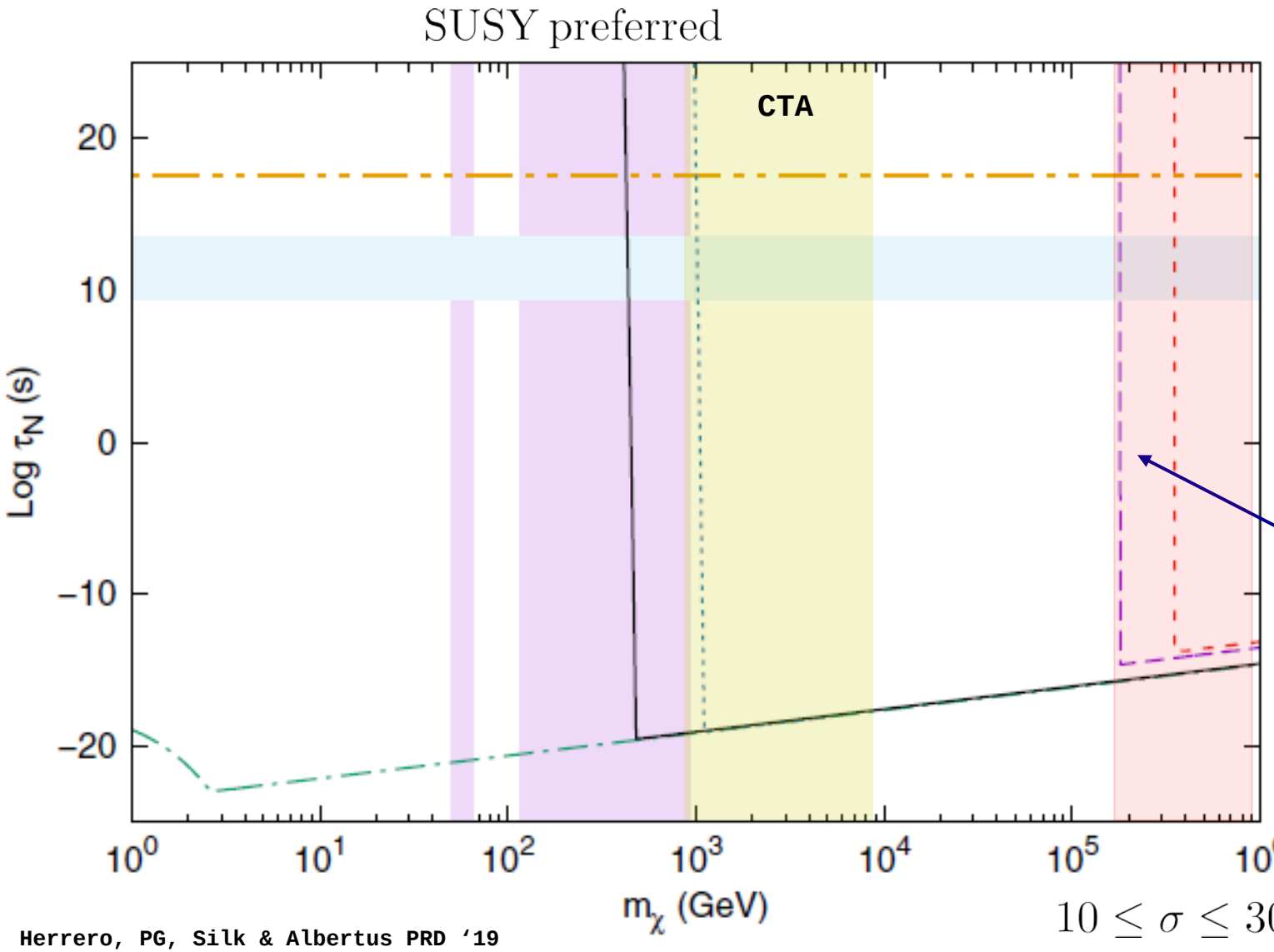

τ_U

$\tau_{\rm NS}$ *ages*

Values preferred from chiral models, QCD and NS masses

$10 \leq \sigma \leq 30\,{\rm MeV\,fm^{-2}}$

$70 \leq B \leq 150\,{\rm MeV\,fm^{-3}}$

Herrero, PG, Silk & Albertus PRD '19

Yet DM: axion-like particles inside NS

Considering a magnetized NS

$$B(n) = B_s + B_0(1 - e^{-\beta(\frac{n}{n_0})^{\delta}})$$

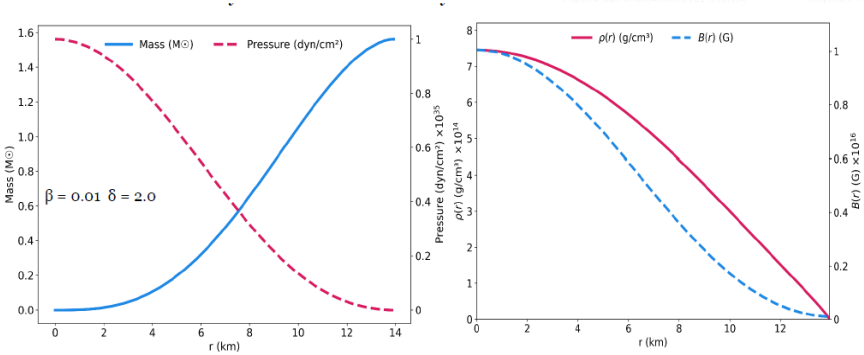

$$\Box a + m_a^2 a = \frac{g_{\gamma,a}}{4} Q \longleftarrow Q(F_0, G_0) \equiv \begin{cases} G_0 & \text{(pseudoscalar coupling)} \\ F_0 & \text{(scalar coupling)} \end{cases}$$

$$F_{\mu\nu}\tilde{F}^{\mu\nu} = -4\,\mathbf{E}\cdot\mathbf{B}$$

Minimal coupling with gravity and electromagnetic source

$$G_0 \equiv -\tfrac{1}{4} F_{\mu\nu}\tilde{F}^{\mu\nu} = \mathbf{E}\cdot\mathbf{B} \quad \text{CP-odd}$$

$$F_0 \equiv -\tfrac{1}{4} F_{\mu\nu}F^{\mu\nu} = \tfrac{1}{2}(\mathbf{E}^2 - \mathbf{B}^2) \quad \text{CP-even}$$

$$\frac{1}{f}\partial_r^2 a + \frac{1}{r^2 k}\partial_\theta^2 a + \tilde{\xi}_1 \partial_r a + \tilde{\xi}_2 \partial_\theta a + m^2 a = g_{\rm eff} Q(F_0, G_0) \qquad g_{\rm eff} \equiv \frac{g_{\gamma a}}{a_0}$$

$$\tilde{\xi}_1(r,\theta) \equiv \frac{\xi_1(r,\theta)}{f(r,\theta)} - \frac{f'(r,\theta)}{f(r,\theta)^2}, \qquad \xi_1(r,\theta) \equiv \frac{2}{r} + \frac{h'}{2h} + \frac{f'}{2f} + \frac{k'}{k},$$

$$\tilde{\xi}_2(r,\theta) \equiv \frac{\xi_2(r,\theta)}{r^2 k(r,\theta)} - \frac{\overset{\circ}{k}(r,\theta)}{r^2 k(r,\theta)}, \qquad \xi_2(r,\theta) \equiv \cot\theta + \frac{\overset{\circ}{h}}{2h} + \frac{\overset{\circ}{f}}{2f} + \frac{\overset{\circ}{k}}{k},$$

Axion-like particles inside NS

Solving the static ALP ode with no field source
(but curved metric)

Boundary condition

$$a(0,\theta) = a_0,$$
$$a(r_{surface},\theta) = a_{sph}(r_{\text{surface}}),$$
$$a(r,0) = a(r,\pi) = a_{sph}(r).$$

$$r_{surface} = \frac{R_e R_p}{\sqrt{R_p^2 \sin^2\theta + R_e^2 \cos^2\theta}},$$

spatially damped oscillator

$$\partial_r^2 a_{sph}(r) + \frac{1}{2}\left(\frac{4}{r} + \nu'(r) - \lambda'(r)\right)\partial_r a_{sph}(r) + m^2 e^{\lambda(r)} a_{sph}(r) = 0.$$

different regimes in the a(r, θ) solution, are determined by the value of the quantity

$$\Delta(r) = \frac{1}{4}\left(\frac{4}{r} + \nu'(r) - \lambda'(r)\right)^2 - 4m^2 e^{\lambda(r)}$$

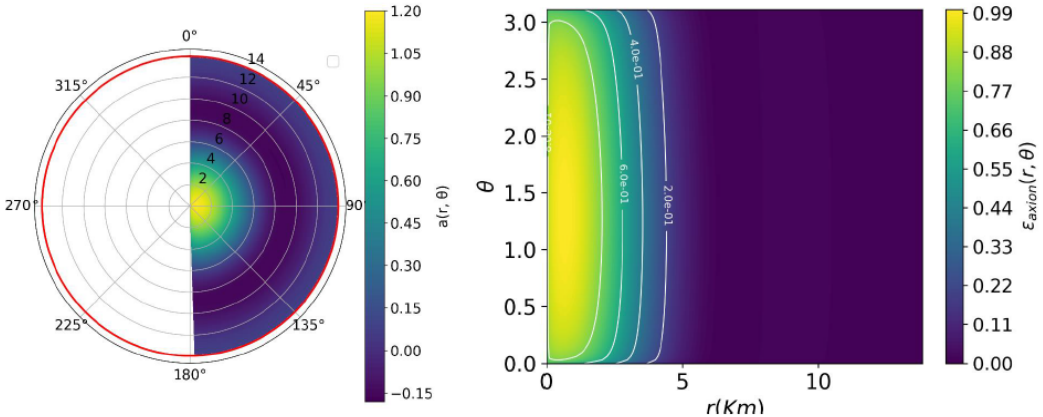

ALP field distribution with a mass $m_a = 10^{-10} eV$ within the interior of the star, presented in an axial cross-section along the polar diameter. The star has a mass $M_{sph} = 1.56\,M\odot$ and a radius R = 13.93 km. The total axion mass was taken to be 0.01% of the total baryonic mass.

Suárez, Albertus and PG submitted

Axion-like particles inside NS

Solving the static ALP ode with axion DM nature:

$$\frac{1}{f}\partial_r^2 a + \frac{1}{r^2 k}\partial_\theta^2 a + \tilde{\xi}_1 \partial_r a + \tilde{\xi}_2 \partial_\theta a + m^2 a = g_{\rm eff}\mathbf{E}.\mathbf{B}$$

chiral magnetohydrodynamics

$$\mathbf{B} = B(\rho)\hat{\boldsymbol{k}}$$

$$\mathbf{E} = \frac{c}{4\pi\sigma}\nabla\times\mathbf{B} - \frac{1}{c}\mathbf{v}\times\mathbf{B} + \underbrace{\frac{e^2}{2\pi^2\sigma\hbar^2 c}\mu_5\mathbf{B}}_{\text{Chiral Magnetic Effect}} + \underbrace{\frac{e\mu_e}{2\pi^2\sigma\hbar^2 c^2}\mu_5\boldsymbol{\omega}}_{\text{Chiral Vortical Effect}}$$

Dehman+25

The combination of strong magnetic fields and chiral asymmetry in particle interactions can lead to a separation of electric charge or axial currents

$$\frac{1}{f(r,\theta)}\partial_r^2 a(r,\theta) + \frac{1}{r^2 k(r,\theta)}\partial_\theta^2 a(r,\theta) + \tilde{\xi}_1(r,\theta)\partial_r a(r,\theta) + \tilde{\xi}_2(r,\theta)\partial_\theta a(r,\theta) + m^2 a(r,\theta)$$
$$= \alpha_1 B(r)^2 + \alpha_2 B(r)\cos(\chi).$$

Suárez, Albertus and PG submitted

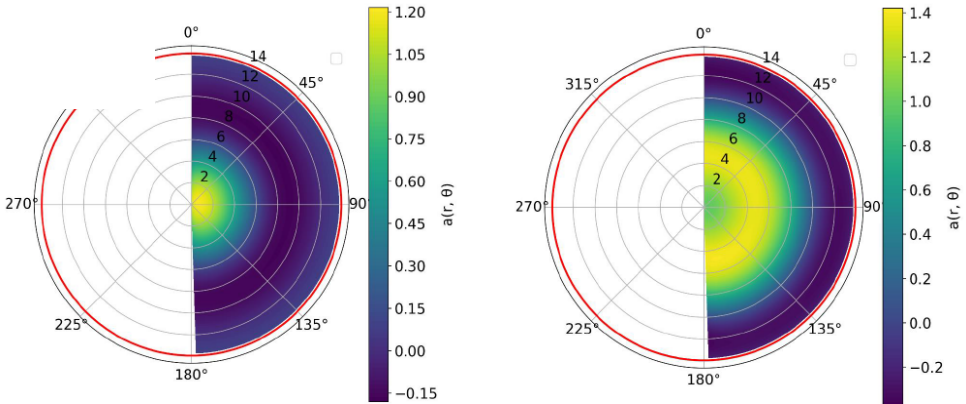

Axion-like particles inside NS

Solving the static ALP ode with SCALAR axion DM nature:

$$\frac{1}{f}\partial_r^2 a + \frac{1}{r^2 k}\partial_\theta^2 a + \tilde{\xi}_1 \partial_r a + \tilde{\xi}_2 \partial_\theta a + m^2 a = g_{\rm eff}(E^2 - B^2)$$

↓ chiral magnetohydrodynamics

$$\frac{1}{f(r,\theta)}\partial_r^2 a(r,\theta) + \frac{1}{r^2 k(r,\theta)}\partial_\theta^2 a(r,\theta) + \tilde{\xi}_1(r,\theta)\partial_r a(r,\theta) + \tilde{\xi}_2(r,\theta)\partial_\theta a(r,\theta) + m^2 a(r,\theta)$$
$$= \beta_1 B^2(r) - 2\beta_2 B(r)\frac{dB(r)}{dr}\sin^2\theta + \beta_2\left(\frac{dB(r)}{dr}\right)^2 \sin^2\theta.$$

$$\beta_1 \equiv g_{\rm eff}\left(-1 + \frac{c^2}{32\pi^2\sigma^2} + \frac{e^4\mu_5^2}{4c^2\pi^4\sigma^2\hbar^2} - \frac{c^2\cos 2\theta}{32\pi^2\sigma^2}\right) \qquad \beta_2 \equiv g_{\rm eff}\frac{c^2}{\sigma^2}$$

We note that for the dominant term, there is an asymmetry factor depending on cos 2θ. We can derive an expression for this asymmetry by comparing the values of β1 along the z-direction and the equatorial direction.

$$F_0[\theta = \tfrac{\pi}{2}] - F_0[\theta = 0] \qquad S_{\rm asym} = \frac{c^2\left(B(r) - \frac{dB(r)}{dr}\right)^2}{16\pi^2\sigma^2}$$

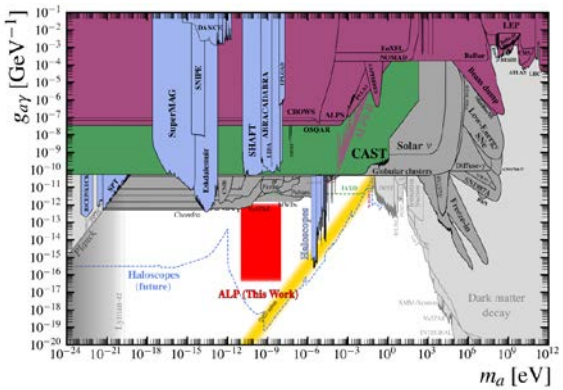

Suárez, Albertus and PG submitted

$$P_{a\to\gamma} = \left(\frac{g_{a\gamma}B_T}{\Delta_{\rm osc}}\right)^2 \sin^2\left(\frac{\Delta_{\rm osc}L}{2}\right)$$

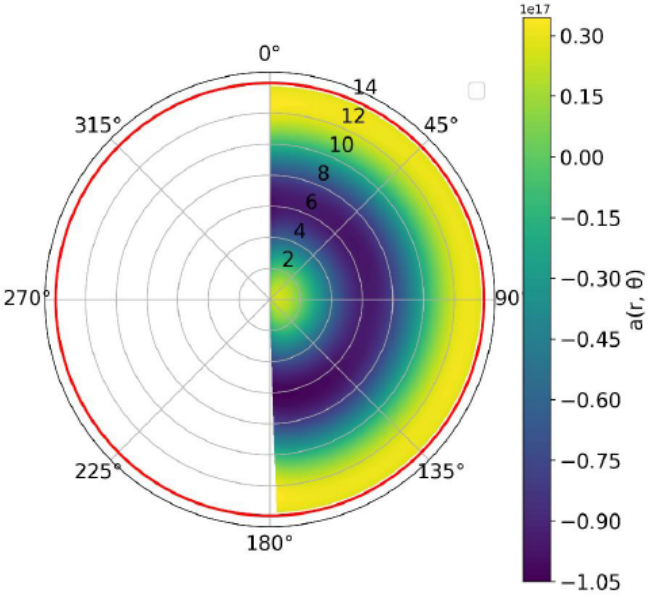

This result is obtained for $m_a = 1 \times 10^{-10} eV$ an axion density equal to 1% of the baryonic density, implying that significant effects arise even at high densities.

Yet many things to understand regarding EoS, so consider also the DARK SIDE as it may be around the corner..